

# **ELECTRIC FIELD IN HEAVY ION COLLISIONS**

A Project Report Submitted

in Partial Fulfilment of the Requirements

for the Degree of

## **MASTER OF SCIENCE**

in

## **PHYSICS**

*by*

**JISHNU N**

**Roll No. 201371**

*Under the supervision of*

**Dr. Suneel Kumar**



*to*

**DEPARTMENT OF PHYSICS AND ASTROPHYSICS**

**CENTRAL UNIVERSITY OF HARYANA**

**MAHENDRAGARH, HARYANA – 123029, INDIA**

**JUNE 2022**



## DEPARTMENT OF PHYSICS AND ASTROPHYSICS CENTRAL UNIVERSITY OF HARYANA

### CANDIDATE'S DECLARATION

I, JISHNU N, hereby declare that my dissertation entitled "**ELECTRIC FIELD IN HEAVY ION COLLISIONS**", submitted at Department of Physics and Astrophysics, School of Basic Sciences, Central University of Haryana, as a partial fulfillment of the requirements for the award of the degree of Master of Science in Physics, is a record of work done by me and not copied from any source without proper citation. This dissertation work has not previously formed the basis for the award of any Degree, Diploma, Fellowship or other similar title or recognition.

I understand the concept of *plagiarism* and declare that while drafting this dissertation I have refrained from plagiarism. I know that plagiarism not only includes direct copying, but also the extensive use of other's ideas without proper referencing or acknowledgment (which includes the proper use of references and quotation marks). If my dissertation is found to be plagiarised at any point of time, I'll be solely responsible and will be ready to accept any decision taken by the competent authority including rejection of my dissertation.

Date: 23/06/2022

Place: MAHENDRAGARH



## DEPARTMENT OF PHYSICS AND ASTROPHYSICS CENTRAL UNIVERSITY OF HARYANA

### CERTIFICATE

This is to certify that the dissertation, entitled "**ELECTRIC FIELD IN HEAVY ION COLLISIONS**", submitted to the Department of Physics and Astrophysics, School of Basic Sciences, Central University of Haryana, as a partial fulfillment of the requirements for the award of the degree of Master of Science in Physics, is a record of review work done by **JISHNU N (201371)** under my guidance. It is further certified that to the best of our knowledge that this dissertation work has not previously formed the basis for the award of any Degree, Diploma, Fellowship or other similar title or recognition at this University or elsewhere.

*S Kumar*

Project Supervisor

**Professor Suneel Kumar**

Dept. of Physics and Astrophysics

Central University of Haryana

*S Kumar*  
23/6/2022

Head of the Department

**Professor Suneel Kumar**

Dept. of Physics and Astrophysics

Central University of Haryana  
Department of Physics  
Central University of Haryana  
Jant-Pali, Mahendergarh

## ACKNOWLEDGEMENT

I want to extend a sincere and heartfelt obligation towards all the personages without whom the completion of the project was not possible. I express my profound gratitude and deep regard to **Dr.Suneel Kumar**, Department of Physics, Central University of Haryana for his guidance, valuable feedback, and constant encouragement throughout the project. I sincerely acknowledge **Mr.Dhanpat Sharma**, PhD scholar, Department of Physics and Astrophysics, Central University of Haryana, for constant support and guidance during the project. I am glad to have got acquaintance with him for he is always kind and patient during all our academic sessions.

I must thank all the faculty members for bestowing me with their knowledge and experience that enabled me to perform my tasks with efficiency and fulfillment. I am also grateful to the Central University of Haryana for allowing me to do this project and providing all the required facilities.

I am immensely grateful to my parents and family for their constant love and blessings without which I cannot achieve any goals in life. Last but not least I thank all my friends who gave moral support and motivation all along our journey together.



JISHNU N

(201371)

## ABSTRACT

The time evolution of internal electric fields in heavy-ion reactions at beam energies between 200 MeV and 600 MeV are studied using Isospin-dependent Quantum Molecular Dynamics (IQMD) model. The variation of electric fields depending on incident beam energies and impact parameter at midrapidity region is discussed by considering  $^{197}_{79}Au + ^{197}_{79}Au$  reaction. The peak values of electric field were observed at around 15 fm/c for 600 MeV beam energy and peaks around 30 fm/c for 200 MeV beam energy. Interestingly, we observe peak mean densities for  $^{197}_{79}Au + ^{197}_{79}Au$  reaction at around 15 fm/c which indicate how anisotropic high density zones correlate to electric field formation. This rise and fall nature of electric field indicates squeeze-out flow observed in transverse direction of reaction plane.

# Contents

<b>Declaration</b>	<b>ii</b>
<b>Certificate</b>	<b>iii</b>
<b>Acknowledgement</b>	<b>iv</b>
<b>Abstract</b>	<b>v</b>
<b>List of figures</b>	<b>viii</b>
<b>1 Introduction</b>	<b>1</b>
1.1 Heavy-Ion Collisions . . . . .	1
1.2 Multifragmentation . . . . .	4
1.3 Phase-space . . . . .	5
1.4 Density profile . . . . .	6
1.5 Electric field generated in HIC . . . . .	7
1.6 Mid-rapidity region . . . . .	8

1.7	Squeeze-out flow . . . . .	9
<b>2</b>	<b>Methodology</b>	<b>11</b>
2.1	Introduction .....	11
2.2	Isospin dependent Quantum Molecular Dynamics (IQMD) model.....	11
2.2.1	Initialization .....	12
2.2.2	Propagation .....	13
2.2.3	Nucleon-Nucleon collision.....	14
<b>3</b>	<b>Results and discussion</b>	<b>16</b>
3.1	Time evolution of Mean Density of system .....	16
3.2	Mean density variation with impact parameter .....	18
3.3	Electric field generated in HIC.....	19
3.3.1	Incident Energy dependence .....	19
3.3.2	Impact parameter dependence .....	21
<b>4</b>	<b>Summary</b>	<b>23</b>
<b>References</b>		<b>25</b>

# List of Figures

1.1	<i>Illustration of heavy ion collisions at intermediate incident energies [1].</i>	3
1.2	<i>Time evolution of heavy-ion collision [2].</i>	6
1.3	<i>Elliptical flow for asymmetric collision in the reaction plane [3].</i>	9
1.4	<i>Schematic representation of out-of-plane flow in reaction plane [3].</i>	10
3.1	<i>Evolution of mean density as function of time at different incident energies.</i>	17
3.2	<i>Evolution of mean density as function of impact parameter.....</i>	18
3.3	<i>Time Evolution of Electric field in transverse direction at midrapidity at different incident energies. ....</i>	20
3.4	<i>Time Evolution of Electric field in transverse direction at midrapidity with varying impact parameter .....</i>	22

# **Chapter 1**

## **Introduction**

### **1.1 Heavy-Ion Collisions**

Nuclear physics have been advancing day by day probing into domain of quantum particles and the applications it opens up to us is unfathomable. Integration of fields like nanotechnology and its applications in material science is evident example of the growth of nuclear physics. Now it is possible to create new form of matter ‘AB-matter’ using femtotechnology, which shows extraordinary properties much better than conventional molecular matter [1]. The ordinary (non-degenerate) matter have huge empty spaces between nucleons and electrons inside any atom. If such a state of matter is obtained through compression, overwhelming all repulsive forces and encompassing all particles into nucleus, it is known as degenerate matter. This matter is only known to exist in stable form in massive celestial objects like blackholes or neutron stars. These stable degenerate matter is called A-B matter which could be synthesised through the advent of femtotechnology. Nanotechnology manipulates matter in the size range of nanometer ( $10^{-9}$  m) whereas femtotechnology operates with matter in size range of femtometer ( $10^{-15}$  m). This form of matter is only accessible through the strong nuclear force observed in nucleons rather than electromagnetic forces in ordinary

matter. Thus its necessary to study nuclear collision at intermediate energies (incident energy between 10 MeV/nucleon to 2 GeV/nucleon) so that by understanding the behaviour of particles during multifragmentation can aid us in production of synthetic degenerate matter required for the production of A-B matter. Moreover we are still in process of developing high energy particle accelerators and thus studies in intermediate energy range is more accessible to experimentation.

The term Heavy ions is provided to those nuclei heavier than Helium nuclei ( $A \geq 4$ ). In these reactions due to interaction between nuclear force fields of colliding nuclei pave way for various nuclear phenomenons which has applications in different fields. From the discovery of nucleus in 1911 by E.Rutherford based on 1909 Geiger-Marsden gold foil experiment [2, 3], we have come a long way. Modern Technology enabled us to extend our domain knowledge from inter-nucleus collisions to collisions between nucleons and finally in understanding quark-gluon plasma, a state attained through strong interaction between partons. This progress can be correlated to development of particle accelerators capable of acceleration ions in various energy ranges. Based on incident energies, heavy ion collisions(HIC) can be classified as Low energies, Intermediate energies and High energies.

Low energy HICs are those collisions with incident energies,  $E \leq 10$  MeV/nucleon. These interactions display some semi-classical features wherein the assumption that ion moves in classical orbits will be valid in most cases. At these energies heavy ion interaction only occurs through their Coulomb or electrostatic fields. Scattering can be elastic based on Rutherford's formula or inelastic by exciting lower nuclear states [4].

High energy HICs are collisions with incident energies,  $E > 2.0$  GeV/nucleon. This energy is required since mass of nucleons are  $0.938$  GeV/c ( $\sim 1$  GeV) and thus to study quark gluon plasma (QGP); this state of matter is achieved at these high energy collisions. QGP is the first complex matter that originated in big bang and from this super hot composition all nucleons came into existence. In a span of  $1$  fm/c, all matter and entropy formed in a HIC assembles into a droplet of strongly coupled QGP, which evolves according to relativistic hydrodynamics with minimal specific viscosity [5]. Further increasing incident energies provide us clues

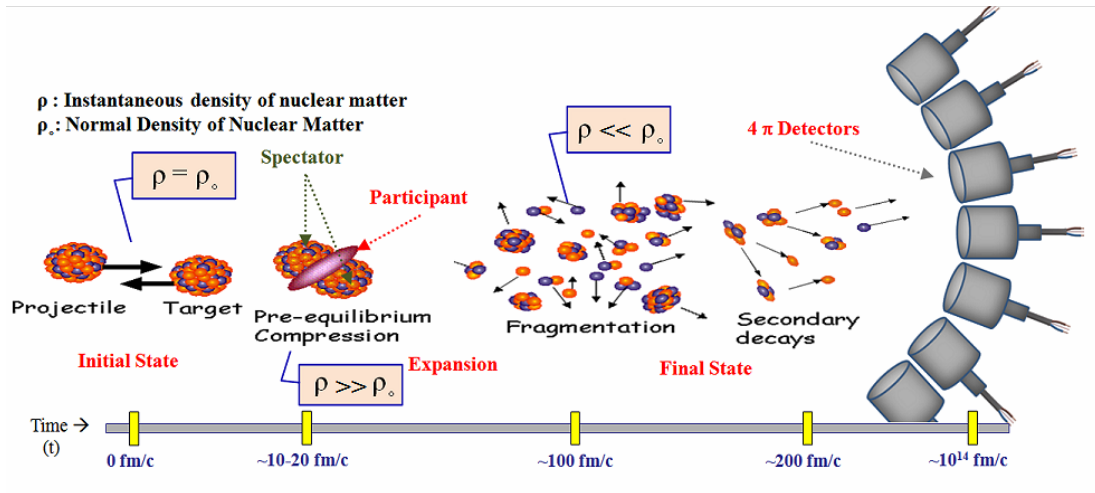


Figure 1.1: Illustration of heavy ion collisions at intermediate incident energies [6].

as to how fundamental particles interact and their structure as well as configurations.

Intermediate energy HICs have incident energies ranging between 10 MeV/nucleon to 2 GeV/nucleon. These energies allow us to study nuclear matter under maximal density and temperature parameters. This highly dense and hot state of matter has densities ( $\rho$ ) multiple times that of normal nuclear density ( $\rho_0 \approx 0.17 \text{ fm}^{-3}$ ). Fragments having mass range between  $2 < A < 30$  stem from the surface of the system and these separate from the rest system when collision density is highest. The number of these clusters ejected decrease as a function of impact parameter. Also a compound-nucleus-like structure forms which emits nucleons and this decay can yield fragments with masses down to  $A = 40$  [7]. The different stages of HIC can be explained using Fig(1.1). At 0 fm/c before collision the density of nuclei is  $\rho_0$ . The instantaneous density of condensed matter,  $\rho$  increases up to 3 times  $\rho_0$  during  $t \approx 10 - 20 \text{ fm}/c$ . This stage is described as pre-equilibrium state or condensed state. This condensed nuclear matter expands leading to  $\rho$  decreasing drastically even less than  $\rho_0$  at around  $t = 100 \text{ fm}/c$ . This stage is called as fragmentation part. Some fragments are highly excited that lead to secondary emissions and others cooldown at around  $t = 200 \text{ fm}/c$ . The lighter fragments produced are a result of asymmetric decay of compound nucleus and heavier fragments were identified as evaporation residues [8, 9]. These decay fragments are detected by  $4\pi$  array of

neutrons and different charge detectors.

## 1.2 Multifragmentation

When the incident energy of projectile nuclei exceeds the binding energies of both target and projectile nuclei, that collision results in the formation of shattered clusters or ‘fragments’. This phenomenon is termed as multifragmentation. This term was proposed by Bondorf et al. in 1976 [10]. During collision, nucleons in colliding nuclei interact with each other leading to expansion of nuclear matter from high to low pressure region. In mass symmetric collision a spherical distribution of nucleons can be observed whereas in mass asymmetric collision there is no uniform distribution of nucleons. This can be explained because of difference in mass between projectile and target nuclei, the smaller projectile can penetrate through target and thus forming unequal fragments in various special orientations. The surface contribution in the case of lighter nuclei is much larger than heavy nuclei [11]. Heavy nuclei will be compressed highly in collision and thus it leads to faster expansion of compressed matter.

The collision yields an excited system which then breaks into fragments of different masses. This process occurs if incident energy is in range of few Mev/nucleon to few GeV/nucleon. The fragments based on their mass number are described in various categories: (i) Free nucleons(FNs)- those fragments which has 4 fm distance from nearest neighbors [ $A = 1$ ], (ii) Light Mass fragments (LMF) [ $2 \leq A \leq 4$ ], (iii) Medium Mass fragments(MMF) [ $5 \leq A \leq 9$ ], (iv) Intermediate Mass fragments [ $5 \leq A \leq A_{tot}/6$ ] and (v) Heavy Mass fragments (HMF). According to nature of collision various fragments are produced. If central collision occurs due to rapid phase interaction lighter fragments are produced. In the case of peripheral collisions, interaction between colliding nuclei is minimal thus lead to formation of heavier fragments.

Discussing certain factors affecting Multifragmentation, gathered from various studies can be concluded in few points. The system-size dependence is already mentioned above. De-

pendence of nucleon- nucleon cross-section is minimal when momentum dependence is considered and according to asymmetry in system its value increases [11]. Multiplicity exhibited by various fragments follow power law behavior which obeys composite system mass data in various studies. This makes multifragmentation suitable to study Liquid-phase phase (LGP) [12]. Multifragmentation also depends on various entrance channel parameter such as incident energy [13], colliding geometry [14], composite mass [15] and mass-asymmetry of colliding nuclei [16]. N/Z dependence can be considered since reaction with higher N/Z produce more neutrons and less number of charged particles compared to reaction with lower N/Z [17]. Neutron deficient reactions in turn produce heavy fragments [17]. Study carried out in IQMD model suggests that Isospin-dependent cross-section shows its influence on fragmentation in the collision of neutron-rich nuclei and its initial N/Z dependence on FNs, LMFs and IMFs are negligible [18].

### 1.3 Phase-space

Phase space provides all information relating to possible momenta and co-ordinate of nucleons participating in collision. Variations in collision parameters like incident energies of projectile or impact parameter gives rise to various phenomenon's which can be evaluated through phase space. Time evolution in HIC can be explained in following steps:

- (i) Initial Phase: When colliding nuclei approach each other, the repulsive N-N interaction can be observed during early overlapping phase.
- (ii) High density Phase: During overlapping phase, the nature of N-N interaction is undeterministic currently. If incident energy of projectile exceeds velocity of sound( $\sim 331m/s$ ), colliding nuclei at ground state nuclear-matter density, a region of high density is formed where nucleon cannot escape from. Ordinary Many-body effects are also observed.
- (iii) Expansion Phase: In this phase nuclear matter is observed at decreasing temperature and density since central region undergoes expansion. The expansion follows in the direction of region of larger gradients in temperature and density. In transverse direction, initial expan-

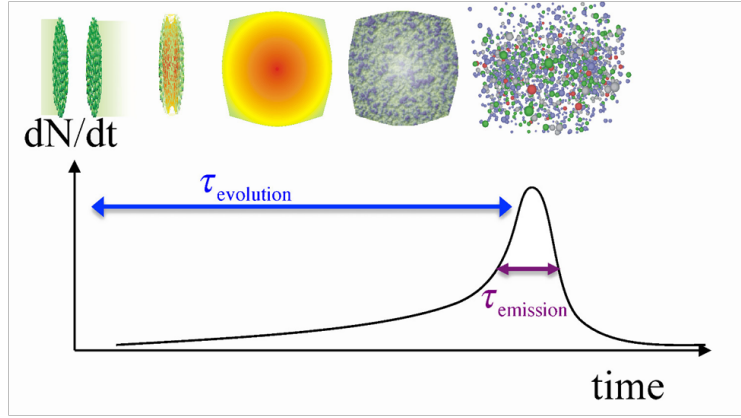


Figure 1.2: *Time evolution of heavy-ion collision [19]*.

sion is primarily towards reaction plane whereas in longitudinal direction, expansion depends on degree of nuclear stopping. For a symmetric central collision, expansion is azimuthally symmetric and for reactions with particular impact parameter having oriented velocity field comes into picture, expansion is much more complex in nature.

(iv) Freeze-Out: The final stage at which reaction comes to a halt at a particular point is regarded as freeze-out region.

## 1.4 Density profile

To obtain total matter density in co-ordinate space, we need to know the wave function associated with every nucleon in the heavy ion system. It is described in classical formalism by a Gaussian wave packet whose width  $\sqrt{L}$  is centered around the mean position  $r_j(t)$  and the mean momentum  $p_j(t)$ , [20]

$$\psi_j(r, t) = \frac{1}{(2\pi L)^{3/4}} \exp \left[ - (r - r_j(t))^2 / 4L \right] \exp [-ip_j(t) \cdot r / \hbar] \quad (1.1)$$

The Wigner distribution of all nucleons is given as,

$$f(r, p, t) = \sum_{j=1}^{A_{\text{total}}} \frac{1}{(\pi \hbar)^3} \exp \left[ -(\mathbf{r} - \mathbf{r}_j(t))^2 / 2L \right] \exp \left[ -(\mathbf{p} - \mathbf{p}_j(t))^2 2L/\hbar^2 \right] \quad (1.2)$$

providing  $L = 1.08 \text{ fm}^2$  to approximate nucleon wave packet size. Total matter density  $\rho(r, t)$  is given as,

$$\rho(r, t) = \sum_{j=1}^{A_{\text{total}}} \rho_j(r, t) = \sum_{j=1}^{A_{\text{total}}} \frac{1}{(2\pi L)^{3/2}} \exp \left[ -(r - r_j(t))^2 / 2L \right] \quad (1.3)$$

This equation defines the number of nucleons present in the proximity of each nucleon in system. In every calculation to find density, we use the position co-ordinate of each nucleon from generated collision data. Also  $r_i(t)$  and  $r_j(t)$  denote corresponding co-ordinate space positions of  $i^{\text{th}}$  and  $j^{\text{th}}$  nucleons respectively.  $L$  is the Gaussian width of wave packet.  $A_{\text{total}}$  represents total number of nucleons present in colliding nuclei. The density is obtained by considering a central sphere having radius  $r = 2 \text{ fm}$  [20]. The density can have two possible values depending on its computation. One way is to calculate  $\langle \rho^{\text{max}} \rangle$  according to maximum value observed in central sphere. Second possibility is calculating  $\langle \rho^{\text{avg}} \rangle$  average densities all over the sphere. Both maximum and average values are equivalent in the case of a uniform distribution of nuclear matter across whole sphere.

## 1.5 Electric field generated in HIC

The significance of electromagnetic fields in our lives needs no further introduction. The process of generating electric fields vary from applying electromotive force between two conducting electrodes to oscillating radio frequency fields using electromagnets in accelerators. Electric fields are used to accelerate charged particles and direct particle beams in accelerators. They are spaced throughout the accelerator, alternating at a given frequency

producing radio waves capable of accelerating beams. It also enables regulation of energy and speed of particle beams. It is observed that in HICs electromagnetic fields are produced by colliding protons. The scale of magnitude of these fields are extremely high compared to those which are produced currently. We focus our study on electric fields generated in HICs and its time evolution based on impact parameter dependence and incident energies in different heavy ions. To calculate electric field at a given position  $\mathbf{r}$  and time  $t$ , the equation is obtained from Liénard-Wiechert potentials [21, 22]

$$e\mathbf{E}(\mathbf{r}, t) = \frac{e^2}{4\pi\epsilon_0} \sum_n Z_n \frac{c^2 - v_n^2}{(cR_n - \mathbf{R}_n \cdot \mathbf{v}_n)^3} (c\mathbf{R}_n - R_n \mathbf{v}_n) \quad (1.4)$$

where  $Z_n$  represent charge number on  $n$ th particle (for proton,  $n = 1$ ),  $\mathbf{R}_n = \mathbf{r} - \mathbf{r}_n$  is the relative position of field point  $\mathbf{r}$  to the source point  $\mathbf{r}_n$ . Here  $\mathbf{r}_n$  is the position of  $n$ th particle with velocity  $\mathbf{v}_n$  at retarded time  $t_n = t - \frac{|\mathbf{r}-\mathbf{r}_n|}{c}$ .

The concept of retarded time is suppose an electromagnetic field is propagated from a source point  $\mathbf{r}_n$  towards an observer at position  $\mathbf{r}$  measuring EM field (at time  $t$ ) will observe a time delay. So retarded time is the actual propagation time  $t_n$  of EM field obtained by substracting time delay from observer's time  $t$ .

The summation for calculation of electric field runs through all charged particles in the system. Considering non-relativistic case  $v \ll c$ , (1.4) reduces to Coulomb's law,

$$e\mathbf{E}(\mathbf{r}, t) = \frac{e^2}{4\pi\epsilon_0} \sum_n Z_n \frac{1}{R_n^3} \mathbf{R}_n \quad (1.5)$$

## 1.6 Mid-rapidity region

The total momentum transfer in a collision is based on participant zone, which is a compressed region of nucleons in the system. All nucleonic flows are originated due to this region. Mid-rapidity region is defined as the region containing compressed nuclear matter.

The rapidity is defined as  $Y^{red} = Y_{c.m.}/Y_{beam}$ ,

where  $Y_{c.m.}$  is given as,

$$Y_{c.m.} = \frac{1}{2} \ln \frac{E(i) + p_z(i)c}{E(i) - p_z(i)c} \quad (1.6)$$

Here,  $E(i)$  and  $p_z(i)$  are the total energy and longitudinal momentum of  $i^{\text{th}}$  particle. The region ( $-0.1 \leq Y_{c.m.}/Y_{\text{beam}} \leq 0.1$ ) is considered as mid-rapidity region and the region past the mid-rapidity conform to spectator zone. Understanding the rapidity distribution of nuclear matter paves way for the study of various nucleonic flows.

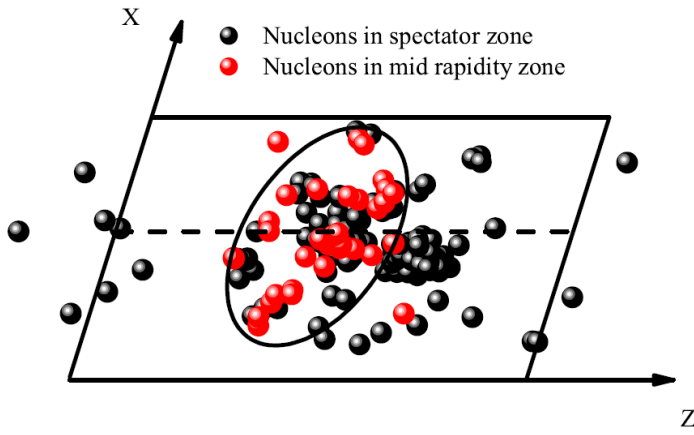


Figure 1.3: *Elliptical flow for asymmetric collision in the reaction plane [23].*

## 1.7 Squeeze-out flow

In the case of non-central collisions, the anisotropy observed in  $\phi$  distribution at midrapidity is visible in the shape of an ellipse fig.1.3 and this flow is described as elliptical flow  $\langle v_2 \rangle$ . Here  $\phi$  is the azimuthal angle between the reaction plane and the transverse momentum of the emitted particle. The red spheres in fig.1.3 shows nucleons present at mid-rapidity region and this distribution of nucleons display ellipse-type behaviour in reaction plane. The particle ejection is out-of-plane ( $v_2 < 0$ ) depending on value of  $\phi$  distribution fig.1.4. Also out-of-plane is obtain if peak of  $\phi$  distribution is at  $\pm 90^\circ$ .

**Out-of-plane squeeze-out flow**  
 $(v_2 < 0)$

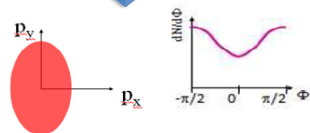
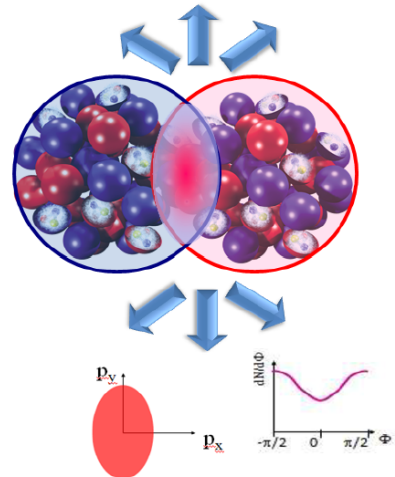


Figure 1.4: *Schematic representation of out-of-plane flow in reaction plane [23].*

# **Chapter 2**

## **Methodology**

### **2.1 Introduction**

From earlier times, many models have been developed to understand heavy ion collision at intermediate energies. One of the successful models able to explain N-body correlations along with nuclear equation of state and also quantum phenomenons like Pauli blocking and particle production, was Quantum Molecular Dynamical (QMD) Model. Later on, an improvisation on this model, providing much more concise experimental results by inclusion of isospin effects was formulated known as Isospin-dependent Quantum Molecular Dynamics (IQMD) model.

### **2.2 Isospin dependent Quantum Molecular Dynamics (IQMD) model**

Isospin-dependent Quantum Molecular Dynamics (IQMD) model is developed from Quantum Molecular Model (QMD) model by including isospin degree of freedom. It is established

by Hartnack et al.[24, 25] and is programmed based on Vlasov Uehling Uhlenbeck (VUU) model. Many studies done on QMD model indicate that it performs well for dynamics of symmetric reactions but fails in the case of asymmetric reactions [26]. But using IQMD model dynamics of most of asymmetric reactions can be studied. IQMD model can also differentiate hadrons like protons, neutrons, delta particle, pions on the basis of charge and isospin state precisely. In this model, by the inclusion of isospin degree of freedom, symmetry potential (thus enabling to study particle distribution in the nucleus), Coloumb interactions between charged particles and isospin-dependent nucleon-nucleon(NN) cross-section comes into picture [27]. In this model each nucleon conform to a Gaussian wave packet. Three steps in this model is described as Initialization, Propagation and N-N collision.

### 2.2.1 Initialization

Nucleons represented as wave packets interact with each other two or three body forces. Since IQMD model generates heavy ion collisions in event-by-event basis all fluctuations and interactions among nucleons will be conserved. Initialisation of nucleons of both projectile and target nuclei are done in rest frame. The centroids of Gaussian in nucleus is distributed in co-ordinate phase sphere of radius given as  $R = R_0 A^{1/3} fm$  where  $R_0 = 1.12 fm$  and also in momentum phase sphere of radius equal to Fermi momentum. Fermi momentum of nucleons is provided by local potential according to relation  $P_f = \sqrt{-2mU(r_i)}$  where  $U(r_i)$  is the local potential and  $r_i$  is position co-ordinate of  $i^{th}$  nucleon. The wave function for  $i^{th}$  nucleon whose mean position co-ordinate is  $r_i(t)$  and mean momentum  $p_i(t)$  is given by,

$$\psi_i(\mathbf{r}, \mathbf{p}_i(t), \mathbf{r}_i(t)) = \frac{1}{(2\pi L)^{3/4}} \exp \left[ \frac{i}{\hbar} \mathbf{p}_i(t) \cdot \mathbf{r} - \frac{(\mathbf{r} - \mathbf{r}_i(t))^2}{4L} \right] \quad (2.1)$$

Here L is the measure of interaction range of nucleus known as gaussian width of system [7]. In IQMD model L is kept system size dependent to attain maximum stability in nucleonic density. Total N-body wave function of reaction system is governed by product of total

coherent states given in eq(2.1) and is represented by  $\Phi$  as,

$$\Phi = \prod_i \psi_i (\mathbf{r}, \mathbf{r}_i, \mathbf{p}_i, t) \quad (2.2)$$

We use wigner formalism to interpret classically described phase-space density distribution. Through this formalism, the reaction dynamics and phase-space dependent observables can be transcribed with ease. Wigner transformation of total coherent states produce a Gaussian-shaped density distribution given as,

$$f_i (\mathbf{r}, \mathbf{p}, \mathbf{r}_i(t), \mathbf{p}_i(t)) = \frac{1}{(\pi\hbar)^3} \exp \left[ \frac{-(\mathbf{r} - \mathbf{r}_i(t))^2}{2L} \right] \exp \left[ \frac{-(\mathbf{p} - \mathbf{p}_i(t))^2 2L}{\hbar^2} \right] \quad (2.3)$$

where  $r_i(t)$  and  $p_i(t)$  implies classical orbit of Gaussian wave packet in time-dependent phase-space. Hence, density of  $i^{th}$  particle in co-ordinate space is given by,

$$\begin{aligned} \rho_i (\mathbf{r}, \mathbf{r}_i(\mathbf{t})) &= \int f_i (\mathbf{r}, \mathbf{p}, \mathbf{r}_i(t), \mathbf{p}_i(t)) d^3 p \\ &= \frac{1}{(2\pi L)^{3/2}} \exp \left[ \frac{-[\mathbf{r} - \mathbf{r}_i(t)]^2}{2L} \right] \end{aligned} \quad (2.4)$$

and density in momentum space is given as,

$$\begin{aligned} g_i (\mathbf{p}, \mathbf{p}_i(\mathbf{t})) &= \int f_i (\mathbf{r}, \mathbf{p}, \mathbf{r}_i(t), \mathbf{p}_i(t)) d^3 r \\ &= \left( \frac{2L}{\pi\hbar} \right)^{3/2} \exp \left[ \frac{-[\mathbf{p} - \mathbf{p}_i(t)]^2 2L}{\hbar^2} \right] \end{aligned} \quad (2.5)$$

## 2.2.2 Propagation

After initialization, the nuclei are projected towards each other through centre of mass velocity based on relativistic kinematics. The propagation of centres of projectile and target is along Coulomb trajectories.

Interactions between nucleons is through two and three-body Skyrme forces, Yukawa po-

tential and Coloumb interactions and an added symmetry potential between nucleons also included [27]. The propagation of hadrons are based on Hamilton's equations of motion given as,

$$\frac{d\vec{r}_i}{dt} = \frac{d\langle H \rangle}{d\vec{p}_i}, \quad \frac{d\vec{p}_i}{dt} = -\frac{d\langle H \rangle}{d\vec{r}_i} \quad (2.6)$$

The total Hamiltonian of system is given as,

$$\begin{aligned} \langle H \rangle &= \langle T \rangle + \langle V \rangle \\ &= \sum_i \frac{\vec{p}_i^2}{2m_i} + \sum_i \sum_{j>i} \int f_i(\vec{r}, \vec{p}, t) V^{ij}(\vec{r}', \vec{r}) \\ &\quad \times f_j(\vec{r}', \vec{p}', t) d\vec{r} d\vec{r}' d\vec{p} d\vec{p}' \end{aligned} \quad (2.7)$$

The baryon potential  $V^{ij}$ , is as follows,

$$\begin{aligned} V^{ij}(|\vec{r}' - \vec{r}|) &= V_{\text{Skyrme}}^{ij} + V_{\text{Yukawa}}^{ij} + V_{\text{Coul}}^{ij} + V_{\text{sym}}^{ij} \\ &= \left[ t_1 \delta(\vec{r}' - \vec{r}) + t_2 \delta(\vec{r}' - \vec{r}) \rho^{\gamma-1} \left( \frac{\vec{r}' + \vec{r}}{2} \right) \right] + t_3 \frac{\exp(|(\vec{r}' - \vec{r})|/\mu)}{|(\vec{r}' - \vec{r})|/\mu} + \frac{Z_i Z_j e^2}{|(\vec{r}' - \vec{r})|} + \\ &t_4 \ln^2 \left[ t_5 \left( \overline{P'} - \overline{P} \right)^2 + 1 \right] \delta[(\vec{r}' - \vec{r}) + t_6 \frac{1}{\rho_0} T_{3i} T_{3j} \delta(\vec{r}'_i - \vec{r}'_j)]. \end{aligned} \quad (2.8)$$

where  $Z_i$  and  $Z_j$  represent charges of  $i^{\text{th}}$  and  $j^{\text{th}}$  baryon,  $t_1$  and  $t_2$  are two and three body coefficients respectively,  $t_3 = -6.66 \text{ MeV}$ ,  $t_4 = 1.54 \text{ MeV}$ ,  $t_5 = 5 * 10^{-4} \text{ MeV}^{-2}$  and  $t_6 = 100 \text{ MeV}$  [28]. Also  $T_{3i}$  and  $T_{3j}$  are isospin projection of  $i^{\text{th}}$  and  $j^{\text{th}}$  particles. The value of  $T_3$  is  $+1/2$  and  $-1/2$  for protons and neutrons respectively.

### 2.2.3 Nucleon-Nucleon collision

The N-N collisions are included in IQMD model using the collision term from well-established VUU-BUU equations [29, 30]. These collisions are carried out stochastically as per cascade models [31, 32]. Parametrisation chosen for N-N scattering cross-sections in IQMD model is that of VerWest and Arndt [33]. During propagation, two nucleons undergoes binary collision

between each other if separation between centroids of gaussian wave packets obey following requirement:

$$|\mathbf{r}_i - \mathbf{r}_j| \leq \sqrt{\frac{\sigma_{tot}}{\pi}}, \quad \sigma_{tot} = \sigma(\sqrt{s}, \text{ type }) \quad (2.9)$$

where 'type' denotes incoming collision partners such as N-N, N- $\Delta$ , N- $\pi$ . Also nucleon-nucleon centre of mass energy is given by,

$$\sqrt{s} = \sqrt{(E_i + E_j)^2 + (P_i + P_j)^2} \quad (2.10)$$

Here  $E_i$  ( $P_i$ ) and  $E_j$  ( $P_j$ ) are the energies of  $i^{\text{th}}$  and  $j^{\text{th}}$  nucleon respectively. The total cross-section is defined as,

$$\sigma^{tot} = \sigma^{el} + \sigma^{inel} = \sigma_{NN}^{el} + \sum_{\text{channels}} \sigma_i^{inel} \quad (2.11)$$

In IQMD model, parameterized free nn, np and pp cross-section is included. It considers all inelastic reaction channels where pions are also formed by decay of  $\Delta$  resonances.

# Chapter 3

## Results and discussion

In this project report, we emphasis on electric field generated in heavy ion collisions and the dependence on intermediate incident energies, variations due to change in impact parameter and time evolution is studied using IQMD model. We primarily focus on heavy ion reaction,  $^{197}_{79}Au + ^{197}_{79}Au$ , for the study of electric field at incident energies- 200 & 600 MeV/nucleon. Also we try to understand how density of collision system evolves over time and this is done by comparing two heavy ion reactions namely,  $^{58}_{28}Ni + ^{58}_{28}Ni$  and  $^{197}_{79}Au + ^{197}_{79}Au$ . A comparison of both these reactions is done based on varying degrees of participation of interacting particles according to impact parameter. Finally we try to understand density correlation in electric fields generated in HICs.

### 3.1 Time evolution of Mean Density of system

First plot is that of scaled density  $\langle \rho / \rho_0 \rangle$  as function of time. We have considered 10 time steps (1, 5, 10, 15, 20, 30, 50, 100, 150, 200 fm/c) corresponding to each phase of reaction. Collision data generated is of 500 runs in simulation. The density plot of both  $^{58}_{28}Ni + ^{58}_{28}Ni$  and  $^{197}_{79}Au + ^{197}_{79}Au$  is given at impact parameter  $\hat{b} = 0$  fig(3.1).

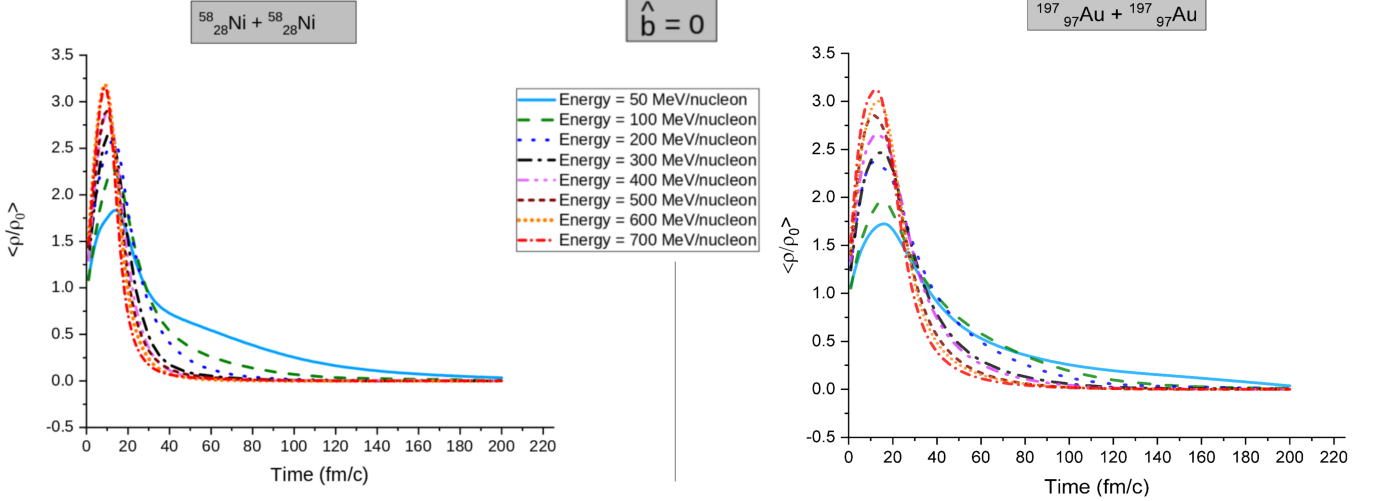


Figure 3.1: *Evolution of mean density as function of time at different incident energies.*

We observe mean density peaks in both  $^{58}_{28}\text{Ni} + ^{58}_{28}\text{Ni}$  and  $^{197}_{79}\text{Au} + ^{197}_{79}\text{Au}$  plots and increase in mean density according to increase in bombarding energies. Since we have considered central collision ( $b=0\text{fm}$ ) at high incident energies, high density zones are formed which is observed as peak values in above plots. As incident energies are increased, anisotropic pressure gradient caused at collision phase also increases which leads to the formation of high density zones. Shortly after, in scattering phase density falls rapidly at high incident energies since interaction time is low in this scenario causing nucleons to move away faster from each other. This is observed in both graphs as sharp negative slope at higher incident energies. Whereas at lower energies, fragment phase-space dominates and thus gradual decrease in mean density is observed due to more interaction time in overlapping of nuclear matter. From the graphs, it is also observed saturation time of mean density is more in the case of  $^{197}_{79}\text{Au} + ^{197}_{79}\text{Au}$  collision compared to  $^{58}_{28}\text{Ni} + ^{58}_{28}\text{Ni}$  collision. It is inferred that saturation time of density depends on mass of colliding nuclei. Massive nuclei takes more time before saturation of mean density.

### 3.2 Mean density variation with impact parameter

From previous plot we observed maximum density attained around 15 fm/c. Here we keep both time  $t = 15 \text{ fm}/c$  and Energy  $E = 600 \text{ MeV/nucleon}$  constant and graph is plotted by varying impact parameter  $b$ .

It is not possible to compare  $^{58}_{28}\text{Ni} + ^{58}_{28}\text{Ni}$  and  $^{197}_{79}\text{Au} + ^{197}_{79}\text{Au}$  on the basis of same impact parameter due to different nuclear sizes and the participant zones vary according to chosen impact parameter. So our study should consider same degree of participation in collision regardless of value of impact parameter. Here we consider degree of participation at 10%, 20%, 40%, 60%, 80% of collision. As degree of participation  $\hat{b}$  increases number of participant nucleons decreases. If  $\hat{b}=0.8$ , it corresponds to 20% of total nucleons acting as participant nucleons in reaction. So plot between mean density of all nucleons vs impact parameter is given in fig(3.2).

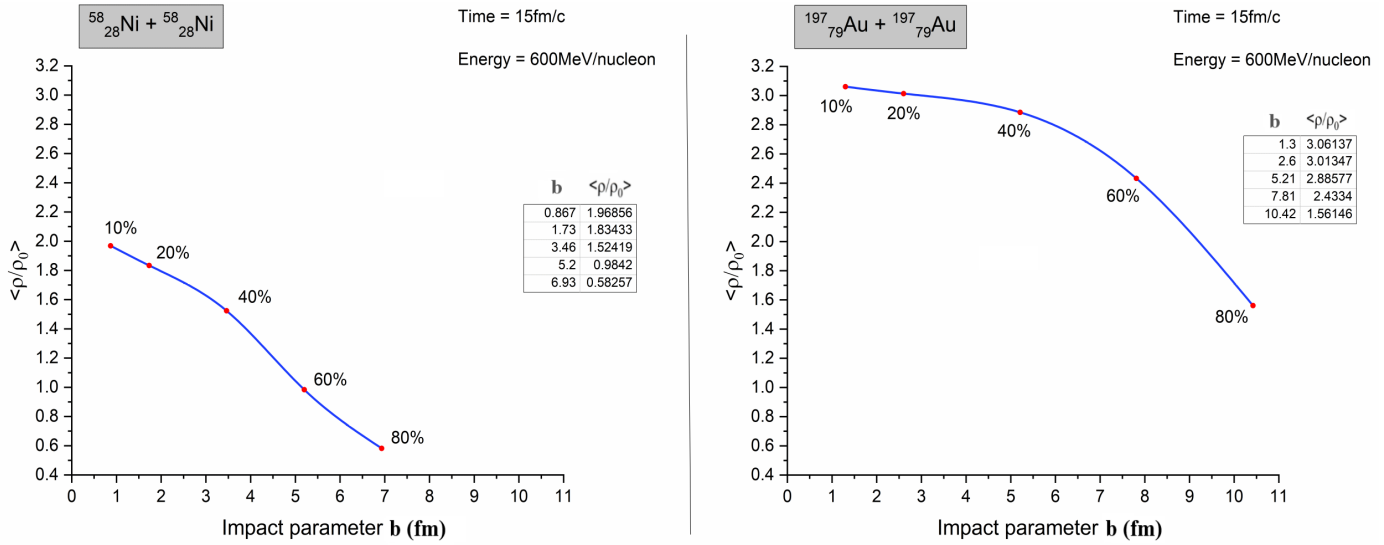


Figure 3.2: Evolution of mean density as function of impact parameter.

We observe that mean density decreases with increase in impact parameter in both cases. As impact parameter increases the nature of collision changes from central to peripheral collisions. The same is suggested in form of degree of participation  $\hat{b}$  which enables us to compare

different nuclei plots. At  $\hat{b} = 0.1$  almost 90% of total nucleons in reaction system act as participant nucleons thus mean density observed in both cases are maximum values. As  $\hat{b}$  increases there are more spectator nucleons than participants which suggest that number of free nucleons decrease in the system and formation light mass and heavy mass fragments will be more. This lack of overlapping zone in reaction is visible as decrease in mean density as impact parameter increases in both plots. The higher magnitude of mean density in  $^{197}_{79}Au + ^{197}_{79}Au$  collision is due to presence of more participant nucleons compared to  $^{58}_{28}Ni + ^{58}_{28}Ni$  collision.

We also observe negative slope in the case of  $^{58}_{28}Ni + ^{58}_{28}Ni$  nuclei collision. Whereas  $^{197}_{79}Au + ^{197}_{79}Au$  nuclei collision shows approximately constant value over a range and then decreasing with increase in  $b$ . In elliptical flow, the maximum squeeze out is observed between semi-central collision to semi-peripheral collision. This squeeze out is associated with pressure gradient in the reaction system leading to the formation of high density zones. This is corresponding to constant range of mean density observed in  $^{197}_{79}Au + ^{197}_{79}Au$  reaction. Further decrease in mean density is due to lack of participant nucleons in peripheral collisions. Now, the sharp negative slope in  $^{58}_{28}Ni + ^{58}_{28}Ni$  nuclei collision is because of less number of participant nucleons in midrapidity zone and with further increase in  $b$ , the number of participant nucleons available for transfer of energy also decreases. The gradual decrease for  $^{197}_{79}Au + ^{197}_{79}Au$  reaction is due to presence of more participants for transfer of energy and more number of participant nucleons is due to higher system mass compared to latter.

Calculation of degree of participation is done as follows: Nuclear radii of  $^{197}_{79}Au \Rightarrow$

$$R = R_0 A^{1/3}$$

$$R = 1.12 * (197)^{1/3} \approx 6.517 \text{ fm} \quad \{R_0 = 1.12 \text{ fm}\}$$

Maximum value of impact parameter  $b_{max} = 2 * R$

$$\text{From, Degree of participation } \hat{b} = \frac{b}{b_{max}}$$

We can calculate the corresponding value of  $b$  for particular degree of freedom.

eg:  $b$  value for 50% participation for  $^{197}_{79}Au$  and  $^{58}_{28}Ni$  is given by,

$$b_{Au} = 0.5 * 13.03 = 6.51 \text{ fm}$$

$$b_{Ni} = 0.5 * 8.67 = 4.33 \text{ fm}$$

### 3.3 Electric field generated in HIC

We primarily focus on electric field produced in transverse plane i.e,  $E_y$  with respect to time. Study is based on  $^{197}_{79}Au + ^{197}_{79}Au$  collision. The electric field  $\mathbf{E}$  is in order of  $10^{23} N/C$ . Time is of units fm/c. Collision data generated under study is of 1000 runs in simulation.

#### 3.3.1 Incident Energy dependence

The first set of plots depict  $eE_y$  vs time at incident energies 200 MeV/nucleon and 600 MeV/nucleon at  $b = 9.1$  fm .

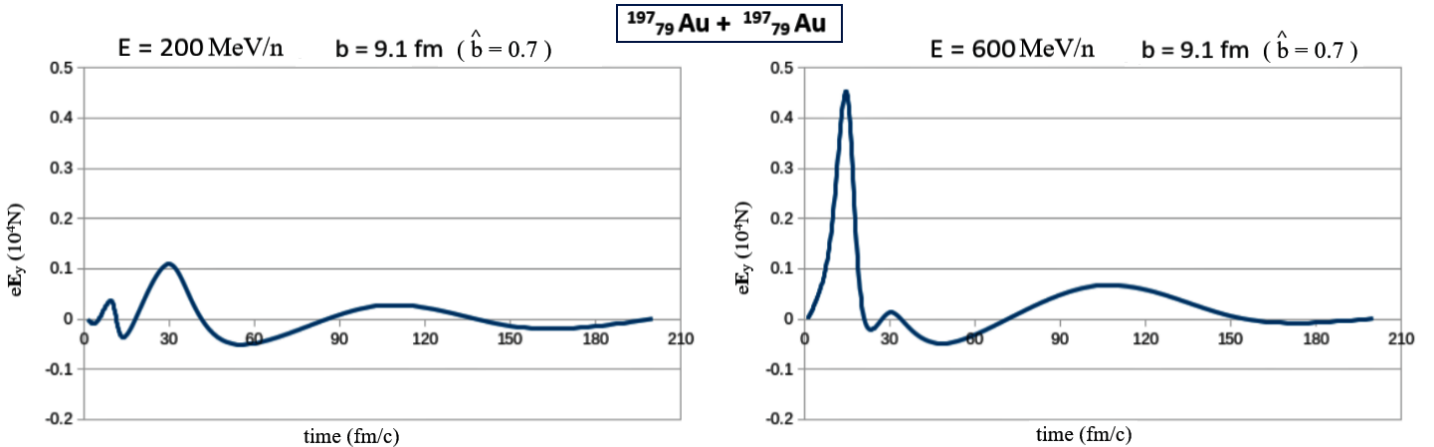


Figure 3.3: *Time Evolution of Electric field in transverse direction at midrapidity at different incident energies.*

We observe peak in electric field strength at  $t=30$  fm/c in the case of low incident energy ( $E=200$  MeV/u) and peak at  $t=15$  fm/c in the case of high incident energy ( $E=600$  MeV/U).The magnitude of  $\mathbf{E}$  at the peak values are  $|\mathbf{E}| = 0.109 * 10^{23} N/C$  and  $|\mathbf{E}| = 0.444 * 10^{23} N/C$  in the case of low energy and high energy respectively. In the case of low energies, interaction time is more between colliding nucleons, thus fragment phase-space dominates in the 'fireball' phase of nuclear collision. This results in peak of  $\mathbf{E}$  to appear at time about 30

fm/c time during the collision. Whereas in the case of high energies, interaction time is less between colliding nucleons, thus nucleon phase space dominates at this phase. This results in peak value of  $E$  observed at early phase of collision (at  $t=15$  fm/c). The influence of mean field is more in case of low energies due to nucleons are constantly interacting with each other but at high energies, nucleon-nucleon collision predominates and the effect of mean field is negligible.

The dependence of maximum value of  $E$  on incident energies is observed. In the case of  $^{197}_{79}Au + ^{197}_{79}Au$  nuclei nuclear matter is large and therefore the number of charged participant nucleons is more. In  $^{197}_{79}Au + ^{197}_{79}Au$  collision an anisotropic high density region is created at collision phase of reaction. At higher incident energies, anisotropy in nuclear matter density is observed due to this high pressure gradient is formed. This pressure gradient formed causes nucleons to start moving from high density to low density zones. This acceleration of nucleons result in production of Electric field. This is associated as squeeze out observed in transverse direction when midrapidity region is under consideration. Depending on high incident energies, the acceleration of nucleons will be high resulting in higher magnitude of  $E$ . Thus we observe higher  $E$  value at 600 MeV/n compared to 200 MeV/n incident energies.

We also observe rapid decrease in maximum value of  $E$  in the case of  $E = 600$  MeV/n compared to  $E = 200$  MeV/n. This is because at higher incident energies after overlapping of nuclear matter in fireball phase, the nucleons retract from each other rapidly. This is observed as sharp negative slope at  $E=600$  MeV/n compared to  $E=200$  MeV/n.

### 3.3.2 Impact parameter dependence

The second set of plots depict  $eE_y$  vs time graphs between  $b=6.51$  fm and  $b=9.12$  fm at fixed incident energy  $E= 600$  MeV/nucleon.

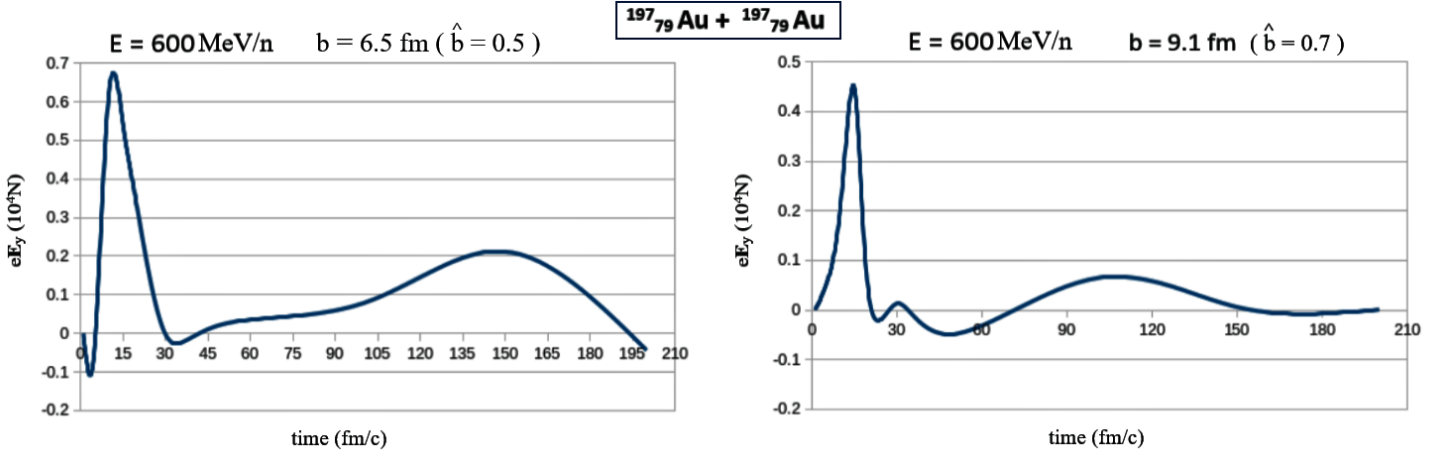


Figure 3.4: *Time Evolution of Electric field in transverse direction at midrapidity with varying impact parameter.*

We observe peaks of electric field strength at around time=15 fm/c in both  $b=6.51$  fm and  $b=9.12$  fm plots at midrapidity. It is evident because incident beam energy is fixed at 600 MeV/n and thus interaction time does not vary and there is no change with varying impact parameter. Also it is evident that maximum value of Electric field strength  $\mathbf{E}$  is higher at lower impact parameter( $b=6.51$  fm) compared to higher impact parameter( $b=9.12$  fm). They correspond to  $\hat{b} = 0.5$  and  $\hat{b} = 0.7$  degree of participation respectively. The maximum values of  $\mathbf{E}$  are  $|\mathbf{E}| = 0.623 * 10^{23} \text{ N/C}$  and  $|\mathbf{E}| = 0.444 * 10^{23} \text{ N/C}$  respectively. At  $\hat{b} = 0.5$  more squeeze out is observed compared to  $\hat{b} = 0.7$ . This is due to more transfer of energy in the case of  $b=6.51$  fm. Hence we get higher magnitude of  $\mathbf{E}$  at lower impact parameter at midrapidity region. In other words, more number of nucleons will be accelerated in transverse direction (y direction) of reaction plane (x-z plane) at  $b= 6.51$  fm compared to  $b= 9.12$  fm.

# Chapter 4

## Summary

In this thesis, the time evolution of electric fields generated in  $^{197}_{79}Au + ^{197}_{79}Au$  reaction is studied. The study was carried out using Isospin-dependent Quantum Molecular Dynamics (IQMD) model. Firstly we introduced Heavy Ion collision and asserted how ‘femtotechnology’ could be the future and how our study of HIC at intermediate energies comes into prominence. Then we followed onto to nuclear phenomenons observed at intermediate energies like multifragmentation and squeeze-out flow at midrapidity region. Also brief review of how phase-space of nucleons are presented in IQMD model is given. We then primarily focus on the concept and mathematical formalism involved in mean density of collision system and electric field generated in HIC. It is followed by a proper discussion on IQMD model which we have considered in our present study. From results, we observed how time evolution of electric field were affected by variation in incident beam energies and impact parameter. It is relevant to observe these variations and range of obtaining extremum fields for nuclear research or even practical applications. The collision data generated from IQMD model was analyzed using a developed python program and graphs were plotted using compiled results.  $eE_y$  vs t graphs of  $^{197}_{79}Au + ^{197}_{79}Au$  collision at different incident beam energies and at different impact parameters were plotted and studied. Time evolution of mean density of  $^{197}_{79}Au + ^{197}_{79}Au$  and  $^{58}_{28}Ni + ^{58}_{28}Ni$  were plotted and compared. The mean density variation

with impact parameter was also studied. The study reveals how squeeze out in transverse direction of reaction plane leads to peak values of electric field strength at midrapidity region. Also by observing mean density variation it is inferred that high electric fields are associated with anisotropic high density regions and acceleration of nucleons from these zones to low density zones. We also observed, how variation in transfer of energy in the reaction system due to impact parameter leads to varying electric field strength at midrapidity region.

# References

- [1] A Bolonkin. Femtotechnology: Nuclear matter with fantastic properties. *Am. J. Eng. Applied Sci*, 2(2):501–514, 2009.
- [2] Hans Geiger. The scattering of  $\alpha$ -particles by matter. *Proceedings of the Royal Society of London. Series A, Containing Papers of a Mathematical and Physical Character*, 83(565):492–504, 1910.
- [3] Ernest Rutherford and Hans Geiger. The charge and nature of the  $\alpha$ -particle. *Proceedings of the Royal Society of London. Series A, Containing Papers of a Mathematical and Physical Character*, 81(546):162–173, 1908.
- [4] PE Hodgson. Heavy ion reactions. *Contemporary Physics*, 23(5):495–512, 1982.
- [5] Wit Busza, Krishna Rajagopal, and Wilke Van Der Schee. Heavy ion collisions: the big picture and the big questions. *Annual Review of Nuclear and Particle Science*, 68:339–376, 2018.
- [6] Anupriya Jain, Suneel Kumar, et al. Influence of isospin dependent nuclear charge radii on fragmentation in heavy ion collisions. *Nuclear Physics A*, 927:220–231, 2014.
- [7] Jörg Aichelin. “quantum” molecular dynamics—a dynamical microscopic n-body approach to investigate fragment formation and the nuclear equation of state in heavy ion collisions. *Physics Reports*, 202(5-6):233–360, 1991.

- [8] C Bhattacharya, D Bandyopadhyay, SK Basu, S Bhattacharya, K Krishan, GSN Murthy, A Chatterjee, S Kailas, and P Singh. Intermediate mass fragments emission in the reaction 96 mev f 19 on c 12. *Physical Review C*, 54(6):3099, 1996.
- [9] Anupriya Jain, Suneel Kumar, et al. Influence of isospin dependent nuclear charge radii on fragmentation in heavy ion collisions. *Nuclear Physics A*, 927:220–231, 2014.
- [10] JP Bondorf. Heavy ion reactions between 30 and a few hundred mev/nucleon. *Le Journal de Physique Colloques*, 37(C5):C5–195, 1976.
- [11] Rajeev K Puri and Jaivir Singh. Multi-fragmentation in heavy-ion collisions: Role of system-size effects, cross-section and equation of state. *Acta Physica Hungarica A) Heavy Ion Physics*, 16(1):233–242, 2002.
- [12] Horst Müller and Brian D Serot. Phase transitions in warm, asymmetric nuclear matter. *Physical Review C*, 52(4):2072, 1995.
- [13] L Phair, W Bauer, DR Bowman, N Carlin, RT de Souza, CK Gelbke, WG Gong, YD Kim, MA Lisa, WG Lynch, et al. Multifragment emission in 36ar+ 197au and 129xe+ 197au collisions. percolation model. *Physics Letters B*, 285(1-2):10–14, 1992.
- [14] CA Ogilvie, JC Adloff, M Begemann-Blaich, P Bouissou, J Hubelle, G Imme, I Iori, P Kreutz, GJ Kunde, S Leray, et al. Rise and fall of multifragment emission. *Physical review letters*, 67(10):1214, 1991.
- [15] Nathalie Marie, A Chbihi, JB Natowitz, A Le Fevre, S Salou, JP Wileczko, L Gingras, M Assenard, G Auger, Ch O Bacri, et al. Experimental determination of fragment excitation energies in multifragmentation events. *Physical Review C*, 58(1):256, 1998.
- [16] J Colin, D Cussol, J Normand, N Bellaize, R Bougault, AM Buta, D Durand, O Lopez, L Manduci, J Marie, et al. Dynamical effects in multifragmentation at intermediate energies. *Physical Review C*, 67(6):064603, 2003.

- [17] Jian-Ye Liu, Yan-Fang Yang, Wei Zuo, Shun-Jin Wang, Qiang Zhao, Wen-Jun Guo, and Bo Chen. Isospin effect on the process of multifragmentation and dissipation at intermediate energy heavy ion collisions. *Physical Review C*, 63(5):054612, 2001.
- [18] Anupriya Jain and Suneel Kumar. Effect of isospin-dependent cross-section on fragment production in the collision of charge asymmetric nuclei. *Pramana*, 78(5):749–758, 2012.
- [19] Mike Lisa. Timescales in heavy ion collisions. *arXiv preprint arXiv:1607.06188*, 2016.
- [20] Dao T Khoa, N Ohtsuka, MA Matin, Amand Faessler, SW Huang, E Lehmann, and Rajeev K Puri. In-medium effects in the description of heavy-ion collisions with realistic nn interactions. *Nuclear Physics A*, 548(1):102–130, 1992.
- [21] Li Ou and Bao-An Li. Magnetic effects in heavy-ion collisions at intermediate energies. *Physical Review C*, 84(6):064605, 2011.
- [22] Wei-Tian Deng and Xu-Guang Huang. Event-by-event generation of electromagnetic fields in heavy-ion collisions. *Physical Review C*, 85(4):044907, 2012.
- [23] Rubina Bansal. Study of correlations between nuclear flow and stopping in heavy ion collisions. 2017.
- [24] Christoph Hartnack, Rajeev K Puri, Jörg Aichelin, J Konopka, SA Bass, Horst Stoecker, and W Greiner. Modelling the many-body dynamics of heavy ion collisions: Present status and future perspective. *The European Physical Journal A-Hadrons and Nuclei*, 1(2):151–169, 1998.
- [25] Sven Soff, Steffen A Bass, Christoph Hartnack, Horst Stöcker, and Walter Greiner. Disappearance of flow. *Physical Review C*, 51(6):3320, 1995.
- [26] Graham F Peaslee, MB Tsang, C Schwarz, MJ Huang, WS Huang, WC Hsi, C Williams, W Bauer, DR Bowman, M Chartier, et al. Energy dependence of multifragmentation in kr 84+ 197 au collisions. *Physical Review C*, 49(5):R2271, 1994.

- [27] Arun Sharma, Rohit Kumar, Samiksha Sood, and Rajeev K Puri. Study of intermediate energy heavy-ion collisions in asymmetric colliding nuclei using computational methods. *International Journal of Pure and Applied Physics*, 13(1):21–25, 2017.
- [28] LG Arnold, BC Clark, ED Cooper, HS Sherif, DA Hutzcheon, P Kitching, JM Cameron, RP Liljestrand, RN MacDonald, WJ McDonald, et al. Energy dependence of the p-ca 40 optical potential: A dirac equation perspective. *Physical Review C*, 25(2):936, 1982.
- [29] P Bonche, S Koonin, and JW Negele. One-dimensional nuclear dynamics in the time-dependent hartree-fock approximation. *Physical Review C*, 13(3):1226, 1976.
- [30] RY Cusson, RK Smith, and JA Maruhn. Time-dependent hartree-fock calculation of the reaction o 16+ o 16 in three dimensions. *Physical Review Letters*, 36(20):1166, 1976.
- [31] Yo Yariv and Zeev Fraenkel. Intranuclear cascade calculation of high-energy heavy-ion interactions. *Physical Review C*, 20(6):2227, 1979.
- [32] Joseph Cugnon. Monte carlo calculation of high-energy heavy-ion interactions. *Physical Review C*, 22(5):1885, 1980.
- [33] Steffen A Bass, Christoph Hartnack, Horst Stöcker, and Walter Greiner. Azimuthal correlations of pions in relativistic heavy-ion collisions at 1 gev/nucleon. *Physical Review C*, 51(6):3343, 1995.